Reduction of Torque Ripple in Induction Motor Drives Using an Advanced Hybrid PWM Technique

Kaushik Basu, J. S. Siva Prasad, G. Narayanan, *Member, IEEE*,
Harish K. Krishnamurthy, and Rajapandian Ayyanar, *Senior Member, IEEE*

***Abstract*—A voltage source inverter-fed induction motor produces a pulsating torque due to application of nonsinusoidal voltages. Torque pulsation is strongly influenced by the pulsewidth modulation (PWM) method employed. Conventional space vector PWM (CSVPWM) is known to result in less torque ripple than sine-triangle PWM. This paper aims at further reduction in the pulsating torque by employing advanced bus-clamping switching sequences, which apply an active vector twice in a subcycle. This paper proposes a hybrid PWM technique which employs such advanced bus-clamping sequences in conjunction with a conventional switching sequence. The proposed hybrid PWM technique is shown to reduce the torque ripple considerably over CSVPWM along with a marginal reduction in current ripple.**

***Index Terms*—Harmonic distortion, induction motor drives, pulsewidth modulated inverters, pulsewidth modulation (PWM), space vector, switching sequence, torque pulsation.**

I. Introduction

SEVERAL pulsewidth modulation (PWM) techniques have been reported for voltage source inverter-fed induction motor drives [1]–[24]. Sine-triangle PWM (SPWM) and conventional space vector PWM (CSVPWM) are popular real-time PWM methods [1]–[3].

Real-time PWM techniques maintain balance between the reference and applied volt–seconds over every subcycle T_s, which is much smaller than the fundamental cycle. As is well known, the commanded reference vector $\mathbf{V_{ref}}$ is synthesized using the two active vectors on either side of it and the zero vector (see Fig. 1). For a reference vector, as shown in Fig. 1, the active states 1 and 2 are applied for durations T_1 and T_2, respectively, as given in (1). The zero vector is applied for the remaining duration T_z [1], [2]

$$T_1 = \frac{V_{\text{ref}} \sin\left(\frac{\pi}{3} - \alpha\right)}{\sin\left(\frac{\pi}{3}\right)} T_s \quad T_2 = \frac{V_{\text{ref}} \sin(\alpha)}{\sin\left(\frac{\pi}{3}\right)} T_s$$
$$T_z = T_s - T_1 - T_2. \tag{1}$$

The zero vector can be applied either using the zero state $---$ (0) or the state $+++$ (7). Continuous modulation schemes such as SPWM and CSVPWM employ both the zero state 0 and state 7 in every subcycle. The inverter state sequence is 0127 (or 7210) when $\mathbf{V_{ref}}$ is in sector I, as shown in Fig. 1. While the division of T_z between the two zero states is unequal in SPWM, it is apportioned equally between the two in CSVPWM, as shown in Fig. 2(a) [2], [4].

Discontinuous PWM (DPWM) methods use only one zero state in a subcycle [1]–[5], [25]. Advanced bus-clamping PWM methods [18]–[21] are similar to DPWM methods in employing only one zero state in a subcycle. However, these techniques apply an active state twice in a subcycle. Fig. 2(b) and (c) shows two of the switching sequences employed by advanced bus-clamping PWM methods. The dwell time of active state 1 is divided into two equal halves in sequence 1012 [Fig. 2(b)], while the active state 2 is applied twice for duration $0.5T_2$ each in sequence 2721 [Fig. 2(c)]. Such

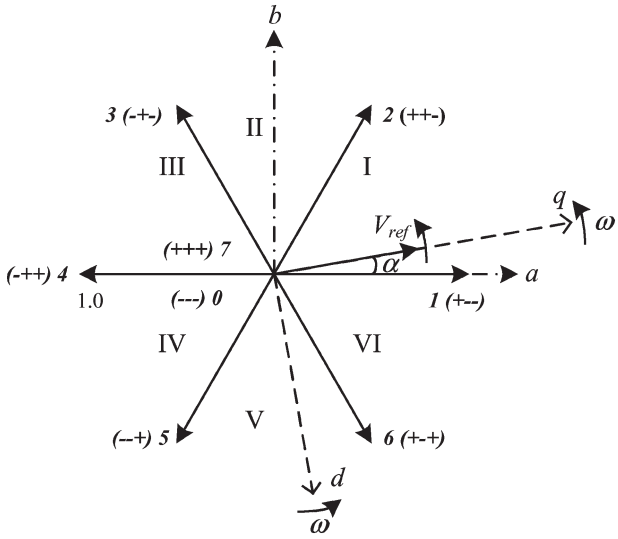

Fig. 1. Voltage vectors of a voltage source inverter normalized with respect to dc bus voltage (I, II, III, IV, V, and VI are sectors).

Manuscript received November 11, 2008; revised March 26, 2009 and May 23, 2009; accepted September 8, 2009. Date of publication October 20, 2009; date of current version May 12, 2010. This work was supported by the Department of Science and Technology, Government of India, under the Science and Engineering Research Council Fast Track Scheme for Young Scientists.

K. Basu was with the Department of Electrical Engineering, Indian Institute of Science, Bangalore 560012, India. He is now with the Department of Electrical Engineering, University of Minnesota, Minneapolis, MN 55455-0213 USA (e-mail: kaushik.iisc@gmail.com).

J. S. Siva Prasad and G. Narayanan are with the Department of Electrical Engineering, Indian Institute of Science, Bangalore 560012, India (e-mail: prasad@ee.iisc.ernet.in; gnar@ee.iisc.ernet.in).

H. K. Krishnamurthy was with the Department of Electrical Engineering, Arizona State University, Tempe, AZ 85287 USA. He is now with Intel Labs, Hillsboro, OR 97124 USA (e-mail: harish.k.krishnamurthy@intel.com).

R. Ayyanar is with the Department of Electrical Engineering, Arizona State University, Tempe, AZ 85287 USA (e-mail: rayyanar@asu.edu).

Digital Object Identifier 10.1109/TIE.2009.2034183

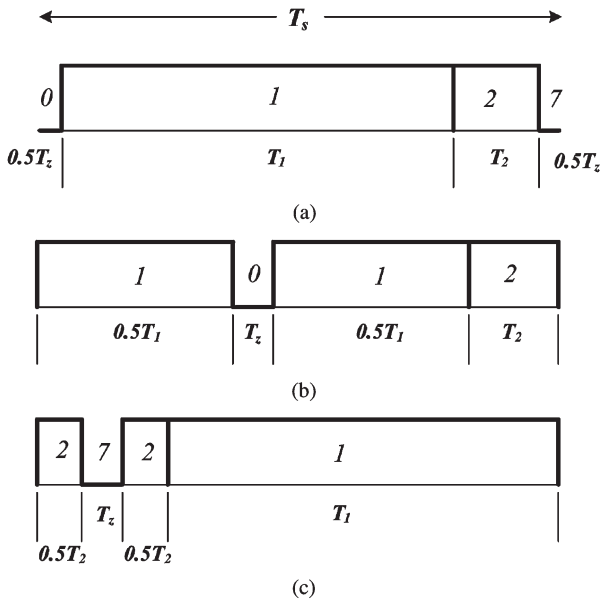

Fig. 2. Switching sequences. (a) 0127. (b) 1012. (c) 2721.

switching sequences are termed variously as *double-switching clamping sequences*, *special sequences*, or *advanced bus-clamping sequences* [18]–[21].

Recently, these special sequences have been shown to be helpful in reducing harmonic distortion in line current as well as inverter switching loss over CSVPWM [20], [21]. This paper investigates the use of such sequences to reduce pulsating torque in inverter-fed induction motor drives.

It should be noted that reduction in torque ripple need not always be accompanied by a corresponding reduction in current ripple. It is possible that a PWM technique might reduce the torque ripple while increasing the current ripple and *vice versa* [16], [18], [19]. Hence, the goal here is to design a PWM technique to reduce torque pulsation without any increase in current ripple, compared to CSVPWM.

II. Current and Torque Ripples

Line current ripple in a PWM inverter is caused by the instantaneous error between the applied and reference voltages [2], [4], [16], [18]. The applied voltage vector at any instant in a subcycle in sector I is either $\mathbf{V_1}$, $\mathbf{V_2}$, or $\mathbf{V_{0,7}}$ [see Fig. 3(a)]. Since the error voltage vector sees the motor as its total leakage inductance, the current ripple vector is proportional to the time integral of the error voltage vector [16], [18].

The current ripple vector can be resolved along the d- and q-axes, which are the reference axes of a synchronously revolving reference frame, as shown in Fig. 3. The current ripple along the d- and q-axes are shown in Fig. 3(b) and (c), respectively, where the quantities Q_1, Q_z, and D are defined as follows:

$$Q_1 = \frac{V_{\rm dc}}{l}\left[\cos(\alpha) - V_{\rm ref}\right]T_1$$

$$Q_z = -\frac{V_{\rm dc}V_{\rm ref}T_z}{l} \quad D = \frac{V_{\rm dc}\sin(\alpha)T_1}{l} \tag{2}$$

where $V_{\rm dc}$ is the dc bus voltage and l is the total leakage inductance of the motor.

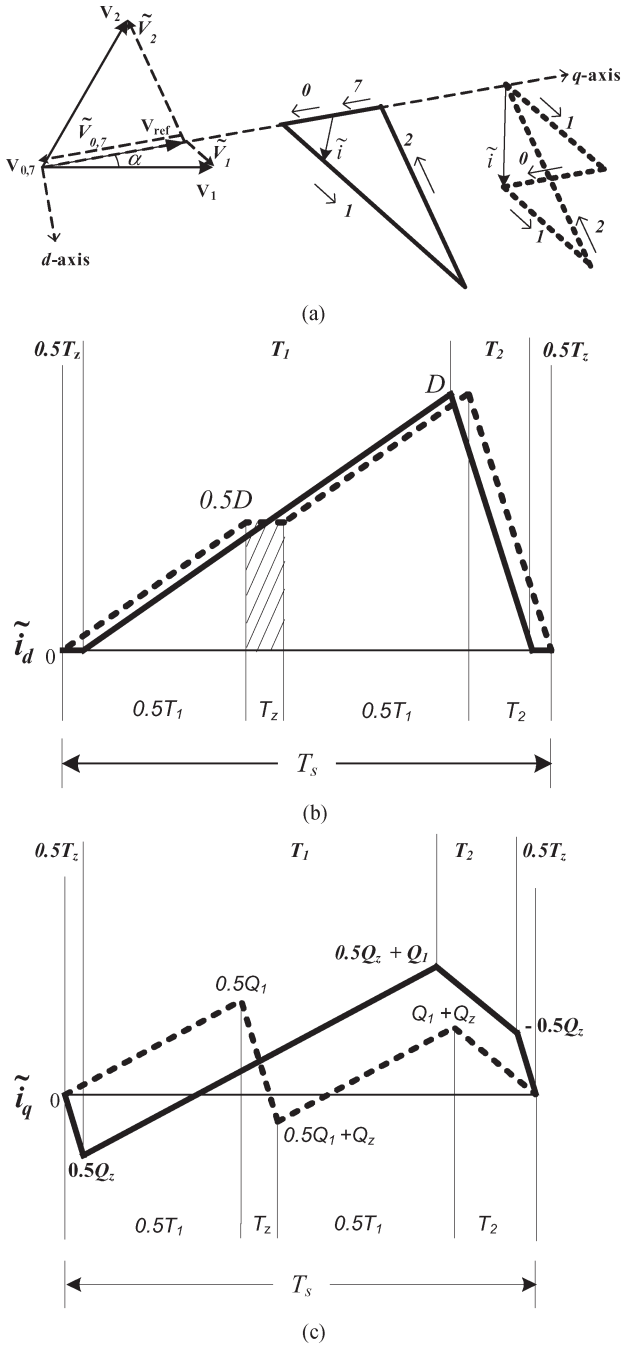

Fig. 3. (a) Trajectory of stator current ripple vector for $V_{\rm ref} = 0.85$ and $\alpha = 10^\circ$. (b) d-axis component of current ripple vector. (c) q-axis component of current ripple vector. (Solid lines) 0127. (Dashed lines) 1012.

Since the voltage reference vector is aligned with the q-axis and the stator resistance drop is negligible, there is a steady flux only along the d-axis. This steady flux interacts with the ripple current along the q-axis to produce the ripple torque. Hence, the torque ripple is practically independent of the d-axis current ripple (since there is no steady flux along the q-axis), while being proportional to the q-axis current ripple as shown in the following:

$$\widetilde{m} = \frac{p}{2}\frac{V_{S1}}{\omega}(1-\sigma)\widetilde{i}_q = K_T\widetilde{i}_q(\text{say}) \tag{3}$$

where p is the number of poles of the machine, V_{S1} is the peak phase fundamental voltage, ω is the fundamental angular frequency, and σ is the ratio of total leakage inductance to magnetizing inductance of the machine [19], [22].

Now, the rms torque ripple over a subcycle $\widetilde{m}_{\rm SUB}$ is proportional to the rms q-axis current ripple $\widetilde{i}_{q,\rm SUB}$ as shown in the following:

$$\widetilde{m}_{\rm SUB} = K_T \widetilde{i}_{q,\rm SUB}. \tag{4}$$

The rms q-axis current ripple over a subcycle can be calculated as indicated in (5a). Similarly, the rms d-axis current ripple and the total rms current ripple over a subcycle can be evaluated as shown in (5b) and (5c), respectively [20]–[22]

$$\widetilde{i}_{q,\rm SUB} = \left[\frac{1}{T_s}\int_0^{T_s} \widetilde{i}_q^2\, dt\right]^{1/2} \tag{5a}$$

$$\widetilde{i}_{d,\rm SUB} = \left[\frac{1}{T_s}\int_0^{T_s} \widetilde{i}_d^2\, dt\right]^{1/2} \tag{5b}$$

$$\widetilde{i}_{\rm SUB} = \sqrt{\widetilde{i}_{q,\rm SUB}^2 + \widetilde{i}_{d,\rm SUB}^2}. \tag{5c}$$

The rms values of torque and current ripples over a subcycle corresponding to sequences 0127, 1012, and 2721 are evaluated and compared in the following section.

III. Proposed Hybrid PWM

For a given reference vector $\mathbf{V_{ref}}$, the rms values of the q-axis current ripple, d-axis current ripple, and total current ripple over a subcycle depend on the switching sequence used.

Fig. 3(b) and (c) shows the d- and q-axes current ripples, respectively, over a subcycle for sequence 0127 (solid lines) and sequence 1012 (dashed lines) for $V_{\rm ref} = 0.85$ and $\alpha = 10^\circ$. From Fig. 3(b), it can be observed that the rms value of the d-axis current ripple with sequence 1012 is greater than that with sequence 0127 [due to the shaded region in Fig. 3(b)]. However, sequence 1012 results in less rms q-axis current ripple than sequence 0127, as shown in Fig. 3(c). Correspondingly, there is a net reduction in the total rms current ripple $(\widetilde{i}_{\rm SUB})$ over the given subcycle with sequence 1012, although only by 7%.

The rms d-axis current ripple $(\widetilde{i}_{d,\rm SUB})$ corresponding to sequence 1012 is higher than that corresponding to sequence 0127 for any $\mathbf{V_{ref}}$. Hence, for certain values of reference vector, it is possible that sequence 1012 might result in a reduced $\widetilde{i}_{q,\rm SUB}$, but an increased $\widetilde{i}_{\rm SUB}$, compared to sequence 0127. However, for any $\mathbf{V_{ref}}$, if sequence 1012 results in a reduced $\widetilde{i}_{\rm SUB}$, it is certain that it would lead to a reduced $\widetilde{i}_{q,\rm SUB}$ as well (as shown by the example in Fig. 3).

An analytical method for comparing the rms current ripple over a subcycle due to any two switching sequences has been discussed in detail in [18], [20], and [21]. An expression for the rms current ripple due to sequence 0127 can be derived based on Fig. 3 (solid lines) and (5). This turns out to be a function of $V_{\rm ref}$, α, and T_s [18], [21]. The rms current ripple over T_s corresponding to sequence 1012 can similarly be expressed in terms of $V_{\rm ref}$, α, and T_s based on Fig. 3 (dashed lines) and (5) [21]. A comparison of the two expressions shows that sequence 1012 leads to lower rms current ripple than sequence 0127 whenever the tip of $\mathbf{V_{ref}}$ falls in region A in Fig. 4. As this reduction in $\widetilde{i}_{\rm SUB}$ in region A happens despite an increase in $\widetilde{i}_{d,\rm SUB}$, sequence 1012 leads to a substantial reduction in $\widetilde{i}_{q,\rm SUB}$ over sequence 0127. Similarly, sequence 2721 leads to reduced rms values of q-axis current ripple as well as total current ripple, compared to sequence 0127, whenever the tip of $\mathbf{V_{ref}}$ falls in region C in Fig. 4. Note that regions A and C are symmetric about the middle of the sector (i.e., $\alpha = 30^\circ$).

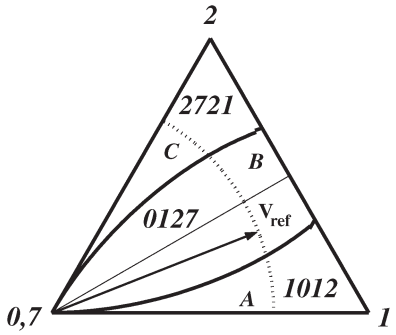

Fig. 4. Proposed RTRHPWM.

Thus, among the three sequences, sequence 0127 leads to the lowest $\widetilde{i}_{\rm SUB}$ for any reference vector in region B. Similarly, sequences 1012 and 2721 are the best in terms of $\widetilde{i}_{\rm SUB}$ in regions A and C, respectively.

The proposed hybrid PWM technique, termed reduced torque ripple hybrid PWM (RTRHPWM), employs the best among the three sequences in terms of $\widetilde{i}_{\rm SUB}$ for any given reference vector. As $\mathbf{V_{ref}}$ sweeps through region A of sector I, sequences 1012 and 2101 are used in alternate subcycles. Similarly, sequences 0127, 7210, ... are employed in region B. Sequences 2721, 1272, ... are used in region C.

While all three phases switch an equal number of times in region B, the number of commutations of the three phases is different in regions A and C. However, the total number of commutations in any subcycle is three in any of the three regions. Hence, the total number of switchings of all the three phases over a sector with the proposed PWM is equal to that with CSVPWM for a given sampling frequency $f_s = (1/T_s)$.

Furthermore, if R-phase "double-switches" over certain duration while $\mathbf{V_{ref}}$ sweeps through region A, the phase is clamped for an equal duration while $\mathbf{V_{ref}}$ passes through region C. Similarly, B-phase "double-switches" in region C, while being clamped in region A. The Y-phase switches once in every T_s throughout the sector. Thus, it can be seen that all three phases switch an equal number of times over a sector. This is equal to the number of commutations per phase per sector with CSVPWM for the same sampling frequency.

The rms torque and rms current ripples due to the proposed technique are compared against those of CSVPWM at a given average switching frequency (i.e., switching frequency averaged over a line cycle) in the following section.

IV. Results and Discussion

The mean-square values of current and torque ripples over a subcycle can be calculated for different sequences, as explained in Section II. These quantities can be averaged over a sector to obtain the respective mean-square values over a sector or a fundamental cycle, as shown in (6a) and (6b), respectively,

$$\widetilde{i}_{\mathrm{rms}} = \left[\frac{3}{\pi}\int_0^{\frac{\pi}{3}} \widetilde{i}^2_{\mathrm{SUB}}\, d\alpha\right]^{1/2} \tag{6a}$$

$$\widetilde{m}_{\mathrm{rms}} = \left[\frac{3}{\pi}\int_0^{\frac{\pi}{3}} \widetilde{m}^2_{\mathrm{SUB}}\, d\alpha\right]^{1/2}. \tag{6b}$$

Being independent of the PWM technique employed, it can be seen that the rms current ripple is proportional to the right-hand side (RHS) of (7a). Similarly, the rms torque ripple corresponding to any PWM technique is proportional to the RHS of (7b). Hence, these two quantities can be regarded as the base values for representing the rms values of current and torque ripples, respectively, as shown in the following [19]:

$$\widetilde{i}_{\mathrm{base}} = \frac{V_{\mathrm{dc}} T_s}{l} \tag{7a}$$

$$\widetilde{m}_{\mathrm{base}} = \frac{V_{\mathrm{dc}} T_s}{l} K_T. \tag{7b}$$

It may be noted that torque ripple as well as current ripple is independent of the slip or the load torque on the motor. These are inversely proportional to the leakage inductance l. The magnetizing inductance impacts the factor K_T in (7b) and (3), thereby influencing the torque ripple. The current ripple, on the other hand, is practically unaffected by the magnetizing inductance. The rms values of current ripple as well as torque ripple are also proportional to the subcycle duration T_s. However, if the ripple quantities are normalized with respect to the base quantities indicated in (7), the normalized values are independent of machine parameters and switching frequency $f_{\mathrm{sw}} = 1/(2T_s)$.

The normalized rms torque ripple corresponding to the proposed RTRHPWM is compared against that of CSVPWM over the entire linear modulation range in Fig. 5(a). Similarly, the rms current ripple due to CSVPWM and that due to the proposed hybrid PWM are shown plotted against V_{ref} in Fig. 5(b).

While the proposed RTRHPWM reduces rms torque ripple compared to CSVPWM over the entire range of modulation, the reduction is significant only for $V_{\mathrm{ref}} > 0.45$, as shown in Fig. 5(a). The best reduction is observed at $V_{\mathrm{ref}} = 0.866$, where the torque ripple reduces by about 23% from 0.0278 to 0.0215 pu. For motor parameters listed in Table I, a dc bus voltage of 283 V and a sampling frequency $(f_s = 1/T_s)$ of 7.2 kHz, the rms torque ripple reduces from 0.746 to 0.578 N · m at $V_{\mathrm{ref}} = 0.866$, with the rated torque of the motor being 19 N · m. Besides the reduction in torque ripple, RTRHPWM also results in a marginal reduction in current ripple over CSVPWM at high modulation indexes, as shown in Fig. 5(b).

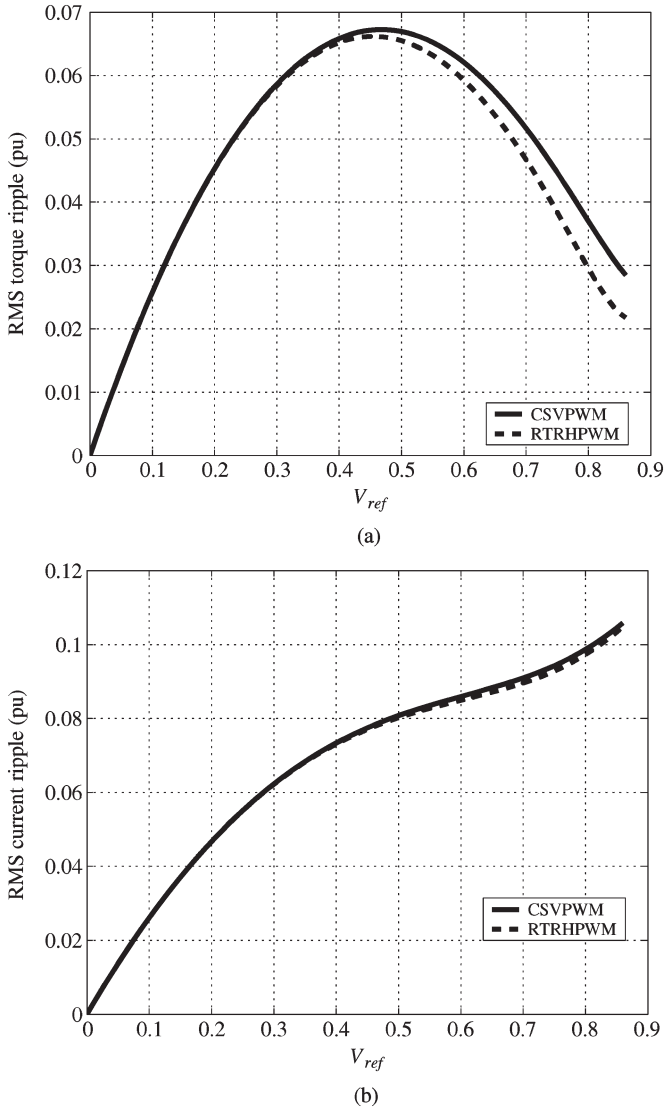

Fig. 5. Comparison of CSVPWM and RTRHPWM. (a) RMS torque ripple. (b) RMS current ripple.

As it is clear from the aforementioned discussion, the current ripple as well as torque ripple can be reduced by increasing the inverter switching frequency f_{sw}. However, the switching frequency cannot be increased beyond a certain limit due to losses in the devices. At any given switching frequency, the proposed technique is capable of reducing the ripple quantities compared to CSVPWM. This is particularly helpful in high-power drives where the switching frequency is limited and the machine leakage inductance is also likely to be low.

The analytical evaluation of $\widetilde{i}_{\mathrm{rms}}$ and $\widetilde{m}_{\mathrm{rms}}$ (presented in Fig. 5) considers a simplified harmonic model of the induction motor, namely, the total leakage inductance. As a next stage of verification, numerical simulations are carried out using a standard motor model [26], which is more detailed than the one considered for analysis. The motor parameters are shown in Table I.

Fig. 6(a) and (b) shows the simulation results of the instantaneous torque ripple for CSVPWM and RTRHPWM, respectively, for $V_{\mathrm{ref}} = 0.84$. The average torque is 2 N · m. As seen, the instantaneous torque ripple has a periodicity of 60°. The

TABLE I
MOTOR PARAMETERS

Output power	3 kW	Rotor resistance	0.94 Ω
Rated speed	1486 RPM	Stator inductance	183 mH
Rated voltage	200 V L-L rms	Rotor inductance	183 mH
Frequency	50 Hz	Mutual inductance	176 mH
Stator resistance	0.94 Ω		

torque ripple is higher toward the start and the end of the sector, compared to the middle of the sector. RTRHPWM results in reduced peak–peak torque ripple compared to CSVPWM (because of application of sequence 1012/2721), which can also be observed in Fig. 3(c). The slope of the q-axis current ripple changes its sign twice over a subcycle duration for sequence 0127, while its sign changes thrice for sequence 1012, as shown in Fig. 3(c). This is reflected in the instantaneous torque ripple waveforms shown in Fig. 6(a) and (b). Around the sector boundaries, the sign of the slope of the ripple torque changes more often in Fig. 6(b) than in Fig. 6(a) due to deployment of sequences 1012 and 2721.

Fig. 6(c) shows the rms torque ripple obtained through simulation for $V_{\rm ref}$ ranging from 0.6 to 0.85 in steps of 0.05. These are in close agreement with the corresponding analytical values [solid and dashed lines in Fig. 6(c)].

CSVPWM and RTRHPWM techniques are implemented and tested on an experimental setup consisting of a 5-kVA-IGBT-based inverter and a squirrel-cage induction motor whose parameters are shown in Table I. The dc bus voltage is 283 V. A TMS320LF2407 DSP-based digital controller is used. The sampling frequency $(1/T_s)$ is 7.2 kHz. The measured current waveforms corresponding to RTRHPWM for $V_{\rm ref} = 0.7$ at a fundamental frequency of 40.4 Hz are shown in Fig. 7.

For a switching frequency of 3.6 kHz, the torque harmonics produced are around 3.6 kHz, 7.2 kHz, ... [19]. Due to bandwidth limitations of commercially available torque sensors, the following procedure [22] is used to obtain the experimental values of rms torque ripple. The motor currents are measured. The motor terminal voltages are obtained using the measured dc bus voltage and the PWM signals, neglecting device drops and the effect of dead time. The motor currents and the terminal voltages are fed to the standard motor model [26] to obtain the instantaneous torque. The average torque over a line cycle is subtracted from the instantaneous torque to get the instantaneous torque ripple, whose rms value is then calculated over a fundamental cycle.

Table II shows the experimental values of rms torque ripple (at an average torque of 2 N · m) and rms current ripple for CSVPWM and the proposed RTRHPWM for $V_{\rm ref} = 0.8$ and 0.85. While analytical and simulation results predict a reduction of about 22% in rms torque ripple at $V_{\rm ref} = 0.85$ [Fig. 6(c)], the experimental results in Table II show a reduction close to 11% only. The difference between the theoretical and the experimental results could be due to device drops and dead-time effect being ignored, besides assumptions made in the machine model. The machine model ignores the dependence of machine parameters on frequency, depth of slots, nonlinearity in magnetic circuit, and distortion in the distribution of magnetomotive force. While such assumptions are valid for

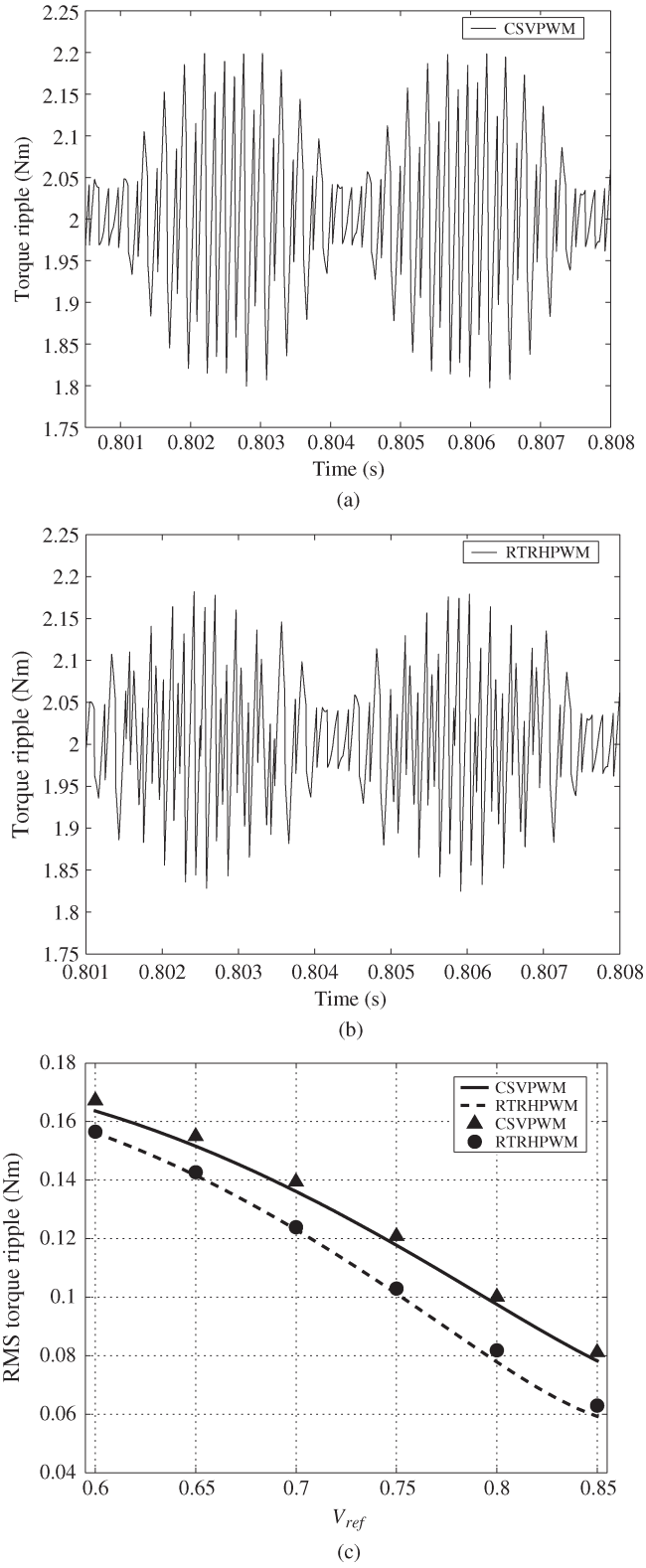

Fig. 6. (a) Simulated instantaneous torque ripple with CSVPWM at $V_{\rm ref} = 0.84$. (b) Simulated instantaneous torque ripple with RTRHPWM at $V_{\rm ref} = 0.84$. (c) Simulated and analytical values of rms torque ripple corresponding to CSVPWM and RTRHPWM.

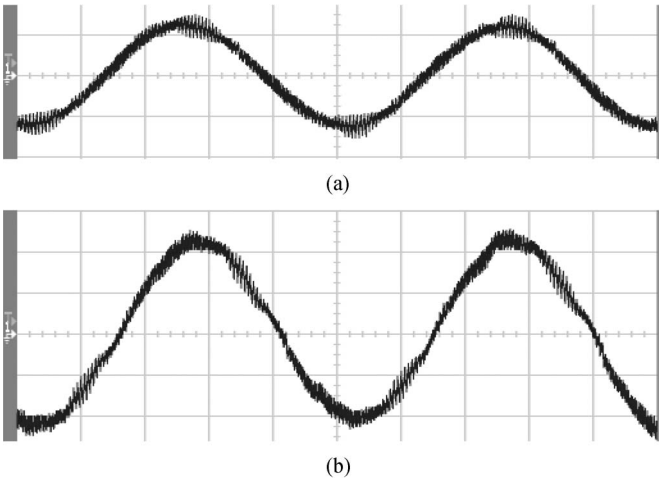

Fig. 7. Experimental line current corresponding to RTRHPWM for $V_{\rm ref} = 0.7$, fundamental frequency of 40.4 Hz, and switching frequency of 3.6 kHz. (a) No load. (b) 70% of full load. Scale: x-axis: 5 ms/division and y-axis: 5 A/division.

TABLE II
EXPERIMENTAL RESULTS

V_{ref}	Torque ripple (Nm)		
	CSVPWM	RTRHPWM	% Reduction
0.8	0.158	0.138	12.6
0.85	0.138	0.123	10.9
	Current Ripple (A)		
	CSVPWM	RTRHPWM	% Reduction
0.8	0.202	0.199	1.49
0.85	0.208	0.206	0.96

computation of average torque, these could lead to significant error while calculating ripple torque [22]. However, all three sets of results—analytical, simulation and experimental—are consistent in demonstrating a substantial reduction in rms torque ripple at high speeds of the drive due to RTRHPWM. In addition to this, RTRHPWM also leads to a marginal improvement in current ripple, as shown in Table II.

V. CONCLUSION

The application of advanced bus-clamping switching sequences for torque ripple reduction in induction motor drives has been studied. A hybrid PWM technique, which is a combination of a conventional sequence and advanced bus-clamping sequences, has been proposed for the reduction of the pulsating torque. Analytical, simulation, and experimental results are consistent in showing a significant reduction in rms torque ripple and a marginal improvement in harmonic distortion of line current due to the proposed hybrid PWM method, compared to CSVPWM, at high speeds of a constant V/f induction motor drive.

REFERENCES

[1] J. Holtz, "Pulse width modulation—A survey," *IEEE Trans. Ind. Electron.*, vol. 39, no. 5, pp. 410–420, Dec. 1992.

[2] D. G. Holmes and T. A. Lipo, *Pulse Width Modulation for Power Converters: Principles and Practice*. Piscataway, NJ: IEEE Press, 2003.

[3] P. G. Handley and J. T. Boys, "Practical real-time PWM modulators—An assessment," *Proc. Inst. Elect. Eng.*, vol. 139, no. 2, pt. B, pp. 96–102, Mar. 1992.

[4] D. Casadei, G. Serra, A. Tani, and L. Zarri, "Theoretical and experimental analysis for the rms current ripple minimization in induction motor drives controlled by SVM technique," *IEEE Trans. Ind. Electron.*, vol. 51, no. 5, pp. 1056–1065, Oct. 2004.

[5] A. Cataliotti, F. Genduso, A. Raciti, and G. R. Galluzzo, "Generalized PWM-VSI control algorithm based on a universal duty-cycle expression: Theoretical analysis, simulation results, and experimental validations," *IEEE Trans. Ind. Electron.*, vol. 54, no. 3, pp. 1569–1580, Jun. 2007.

[6] L. Dalessandro, S. D. Round, U. Drofenik, and J. W. Kolar, "Discontinuous space-vector modulation for three-level PWM rectifiers," *IEEE Trans. Power Electron.*, vol. 23, no. 2, pp. 530–542, Mar. 2008.

[7] A. Mehrizi-Sani and S. Filizadeh, "An optimized space vector modulation sequence for improved harmonic performance," *IEEE Trans. Ind. Electron.*, vol. 56, no. 8, pp. 2894–2903, Aug. 2009.

[8] N. Oikonomou and J. Holtz, "Closed-loop control of medium-voltage drives operated with synchronous optimal pulsewidth modulation," *IEEE Trans. Ind. Appl.*, vol. 44, no. 1, pp. 115–123, Jan./Feb. 2008.

[9] M. H. Bierhoff and F. W. Fuchs, "DC-link harmonics of three-phase voltage-source converters influenced by the pulsewidth-modulation strategy—An analysis," *IEEE Trans. Ind. Electron.*, vol. 55, no. 5, pp. 2085–2092, May 2008.

[10] D. Casadei, G. Serra, A. Tani, and L. Zarri, "Optimal use of zero vectors for minimizing the output current distortion in matrix converters," *IEEE Trans. Ind. Electron.*, vol. 56, no. 2, pp. 326–336, Feb. 2009.

[11] Y. Liu, H. Hong, and A. Q. Huang, "Real-time calculation of switching angles minimizing THD for multilevel inverters with step modulation," *IEEE Trans. Ind. Electron.*, vol. 56, no. 2, pp. 285–293, Feb. 2009.

[12] A. M. Hava and E. Un, "Performance analysis of reduced common-mode voltage PWM methods and comparison with standard PWM methods for three-phase voltage-source inverters," *IEEE Trans. Power Electron.*, vol. 24, no. 1, pp. 241–252, Jan. 2009.

[13] X. Wu, S. K. Panda, and J. Xu, "Effect of pulse-width modulation schemes on the performance of three-phase voltage source converter," in *Proc. 33rd Annu. IEEE IECON*, 2007, pp. 2026–2031.

[14] M. J. Meco-Gutierrez, F. Perez-Hidalgo, F. Vargas-Merino, and J. R. Heredia-Larrubia, "A new PWM technique frequency regulated carrier for induction motors supply," *IEEE Trans. Ind. Electron.*, vol. 53, no. 5, pp. 1750–1754, Oct. 2006.

[15] K. Taniguchi, M. Inoue, Y. Takeda, and S. Morimoto, "A PWM strategy for reducing torque-ripple in inverter-fed induction motor," *IEEE Trans. Ind. Appl.*, vol. 30, no. 1, pp. 71–77, Jan./Feb. 1994.

[16] S. Fukuda and Y. Iwaji, "Introduction of the harmonic distortion determining factor and its application to evaluating real time PWM inverters," *IEEE Trans. Ind. Appl.*, vol. 31, no. 1, pp. 149–154, Jan./Feb. 1995.

[17] Y. Murai, Y. Ghosh, K. Matsui, and I. Hosono, "High-frequency split zero vector PWM with harmonic reduction for induction motor drive," *IEEE Trans. Ind. Appl.*, vol. 28, no. 1, pp. 105–112, Jan./Feb. 1992.

[18] G. Narayanan and V. T. Ranganathan, "Analytical evaluation of harmonic distortion in PWM ac drives using the notion of stator flux ripple," *IEEE Trans. Power Electron.*, vol. 20, no. 2, pp. 466–474, Mar. 2005.

[19] K. Basu, "Minimization of torque ripple in space vector PWM based induction motor drives," M.Sc. (Engg.) thesis, Indian Inst. Sci., Bangalore, India, 2005.

[20] G. Narayanan, D. Zhao, H. K. Krishnamurthy, R. Ayyanar, and V. T. Ranganathan, "Space vector based hybrid PWM techniques for reduced current ripple," *IEEE Trans. Ind. Electron.*, vol. 55, no. 4, pp. 1614–1627, Apr. 2008.

[21] V. S. S. Pavan Kumar Hari and G. Narayanan, "Comparative evaluation of space vector based pulse width modulation techniques in terms of harmonic distortion and switching losses," in *Proc. MCDES*, May 2008. [CD-ROM].

[22] K. Basu, J. S. S. Prasad, and G. Narayanan, "Minimization of torque ripple in PWM ac drives," *IEEE Trans. Ind. Electron.*, vol. 56, no. 2, pp. 553–558, Feb. 2009.

[23] S.-Y. Oh, Y.-G. Jung, S.-H. Yang, and Y.-C. Lim, "Harmonic-spectrum spreading effects of two-phase random centered distribution PWM (DZRCD) scheme with dual zero vectors," *IEEE Trans. Ind. Electron.*, vol. 56, no. 8, pp. 3013–3020, Aug. 2009.

[24] A. Das, K. Sivakumar, R. Ramchand, C. Patel, and K. Gopakumar, "A combination of hexagonal and 12-sided voltage space vector PWM control for IM drives using cascaded two-level inverters," *IEEE Trans. Ind. Electron.*, vol. 56, no. 5, pp. 1657–1664, May 2009.

[25] L. Asiminoaei, P. Rodriguez, and F. Blaabjerg, "Application of discontinuous PWM modulation in active power filters," *IEEE Trans. Power Electron.*, vol. 23, no. 4, pp. 1692–1706, Jul. 2008.

[26] W. Leonhard, *Control of Electrical Drives*, 3rd ed. New York: Springer-Verlag, 2001.

Kaushik Basu received the B.Eng. degree from Bengal Engineering and Science University, Shibpore, India, in 2003, and the M.Sc. (Eng.) degree from the Indian Institute of Science, Bangalore, India, in 2005, both in electrical engineering. He is currently working toward the Ph.D. degree in electrical engineering in the Department of Electrical Engineering, University of Minnesota, Minneapolis.

He was with Coldwatt India Private Limited from 2006 to 2007, where he was responsible for the design and development of high-efficiency power supplies. His major research interests are pulsewidth modulation techniques, motor drives, and magnetic design.

J. S. Siva Prasad received the B.Tech. degree from the SVH College of Engineering, Nagarjuna University, Andhra Pradesh, India, in 2000, and the M.E. degree from the PSG College of Technology, Coimatore, India, in 2002. He is currently working toward the Ph.D. degree at the Indian Institute of Science, Bangalore, India.

He was with the Department of Energy Systems, Indian Institute of Technology, Bombay, India, from 2002 to 2005, and with the Vellore Institute of Technology, Vellore, India, from 2005 to 2006. His research interests are ac drives, pulsewidth modulation, and design of solar converters.

G. Narayanan (S'99–M'01) received the B.E. degree from Anna University, Chennai, India, in 1992, the M.Tech. degree from the Indian Institute of Technology, Kharagpur, India, in 1994, and the Ph.D. degree from the Indian Institute of Science, Bangalore, India, in 2000.

He is currently an Assistant Professor in the Department of Electrical Engineering, Indian Institute of Science. His research interests include ac drives, pulsewidth modulation, multilevel inverters, and protection of power devices.

Dr. Narayanan received the Innovative Student Project Award for his Ph.D. work from the Indian National Academy of Engineering in 2000 and the Young Scientist Award from the Indian National Science Academy in 2003.

Harish K. Krishnamurthy received the M.S. and Ph.D. degrees in electrical engineering from Arizona State University, Tempe.

He is currently a Hardware Development Engineer with Intel Labs, Hillsboro, OR. His research interests include topologies and digital control techniques for switch-mode power converters and new pulsewidth modulation techniques for drives.

Rajapandian Ayyanar (M'00–SM'06) received the M.S. degree from the Indian Institute of Science, Bangalore, India, and the Ph.D. degree from the University of Minnesota, Minneapolis.

He is currently an Associate Professor at Arizona State University, Tempe. His current research interests include topologies and control methods for switch-mode power converters, fully modular power system architecture, new pulsewidth modulation techniques, design of power conversion systems and distribution systems for large scale applications, distributed integration of renewable energy resources (mainly solar photovoltaics and wind), and power electronics applications in enabling "smart grid."

Dr. Ayyanar received the ONR Young Investigator Award in 2005. He is an Associate Editor of the IEEE TRANSACTIONS ON POWER ELECTRONICS.